

An energy-conserving dose summation method for dose accumulation in radiotherapy

Hualiang Zhong

Department of Radiation Oncology, Medical College of Wisconsin, Milwaukee, Wisconsin, USA

Correspondence

Hualiang Zhong, Department of Radiation Oncology, Medical College of Wisconsin, Milwaukee, WI, USA.

Email: hzhong@mcw.edu

Funding information

National Institute of Biomedical Imaging and Bioengineering, NIH, Grant/Award Number: R01-EB032680

Abstract

Background: Radiation therapy often requires the accumulation of doses from multiple treatment fractions or courses for plan evaluation and treatment response assessment. However, due to underlying mass changes, the accumulated dose may not accurately reflect the total deposited energy, leading to potential inaccuracies in characterizing the treatment input.

Purpose: This study introduces an energy-conserving dose summation method to calculate the total dose in scenarios where patients experience changes in body mass during treatment.

Methods and materials: The proposed method transfers dose and mass data from dosimetry images, where the delivered doses were calculated, to a reference image using an energy and mass-conserving dose reconstruction technique. The reconstructed dose assumes the same resolution and dimension as the reference image. The transferred masses are averaged at each image voxel in the reference image to generate an average mass. The transferred doses are then adjusted by multiplying by the ratio of their transferred mass to the average mass, and subsequently summed to calculate a mass-weighted (MW) total dose at each voxel. This method is demonstrated with a case of lung cancer retreatment.

Results: The MW total dose was shown to be equivalent to the total deposited energy divided by the average mass. In the lung cancer retreatment case, the energy derived from the MW total dose was consistent with the sum of energy transferred from two treatments across all evaluated organs.

Conclusion: The MW dose summation method can produce a total dose that accurately reflects the total energy deposited in each organ. The consistency may provide a robust foundation for verifying dose accumulations in adaptive radiotherapy.

KEYWORDS

adaptive radiotherapy, dose accumulation, energy transfer, mass variation, quality assurance

1 | INTRODUCTION

An optimal treatment plan for adaptive radiotherapy or patient retreatment can be effectively developed by incorporating previously delivered doses. These doses usually are calculated on different image frames, and therefore are required to be added to a consensus image through deformable dose accumulation (DDA).¹ DDA involves three basic operations: (1) performing deformable image registration (DIR), (2) translating

doses to a reference image, and (3) summing the translated doses to obtain a total dose. A variety of techniques have been developed for DIR, including Demons,² B-spline,³ mechanical modeling,⁴ and hybrid finite element methods,⁵ and the performance of these algorithms has been evaluated in different studies.⁶ With DIR-generated deformation maps, doses calculated on different images can be translated to a reference image using methods such as dose interpolation,⁷ voxel tracking,⁸ or energy transfer method.⁹

To address the impact of mass changes on dose translation, an energy and mass-conserving (EMC) dose reconstruction method was introduced to translate doses calculated with Monte Carlo¹⁰ and model-based¹¹ dose engines. Its computation speed was improved with GPU-based interpolations¹² and volumetric mapping techniques.¹³ The EMC dose reconstruction was shown to be superior to the dose interpolation method¹⁴ and recommended for MR-guided adaptive radiotherapy.² The energy conservation property inherent in EMC was also used for validation of DIR and dose mapping operations.^{15,16}

In addition to the impact on dose translation, mass changes also compromise dose summation in the reference image. Radiotherapy outcomes ultimately depend on the total radiation energy deposited in the tumor and surrounding tissues. We assume that the goal of dose summation is to determine a total dose that accurately reflects the total deposited energy. Unlike traditional dosimetry, where radiation dose and energy are interchangeable due to static mass, dose summation involves doses calculated on varying masses, and the total dose directly summed from these doses cannot be converted to the total deposited energy. The lack of correspondence to the total deposited energy undermines the validity of using the directly summed total dose for evaluating treatment outcomes.¹⁷

This study aims to present a mass-weighted dose summation (MDS) method that accounts for underlying mass variations, ensuring consistency between the summed dose and the total deposited energy. This consistency not only ensures that the summed total dose accurately reflects the underlying physics, validating its role in treatment outcome assessment, but also provides a direct method for verifying DDA, the uncertainty of which has been a major concern in adaptive radiotherapy.¹⁸

2 | METHODS

2.1 | Dose summation methods

Suppose M_i is a mass image calculated from a CT image X_i acquired at fraction i , and D_i is a dose distribution calculated on X_i , $i = 1, \dots, K$, where K is the number of fractions. φ_i is a transformation map from X_i to a reference image R, and $\varphi_i(M_i)$ is the transferred mass image from X_i to R. A mass-weighted total dose at voxel v can be calculated by

$$D_T(v) = \sum_{i=1, \dots, K} \lambda_i(v) \tilde{D}_i(v) \quad (1)$$

where $\lambda_i(v) = \frac{\varphi_i(M_i)(v)}{M_A(v)}$, M_A is the average mass image calculated by $M_A(v) = \sum_{i=1, \dots, K} \varphi_i(M_i)(v)/K$. $\tilde{D}_i(v)$ is the

transferred dose from X_i to voxel v in R. When there is no mass change in these images, $\lambda_i(v) = 1$ and the dose in Equation (1) becomes the directly summed total dose

$$D_T(v) = \sum_{i=1, \dots, K} \tilde{D}_i(v) . \quad (2)$$

Recall that in the EMC dose reconstruction method, the transferred dose \tilde{D}_i at voxel v is defined as the transferred energy divided by the transferred mass, that is, $\tilde{D}_i(v) = \varphi_i(E_i)(v)/\varphi_i(M_i)(v)$, where $\varphi_i(E_i)$ and $\varphi_i(M_i)$ are the transferred energy and mass on the reference image R. In this case, the term $\varphi_i(M_i)(v)$ in $\lambda_i(v)$ and $\tilde{D}_i(v)$ is cancelled in Equation (1). The total dose in Equation (1) becomes the ratio of the total deposited energy and the averaged mass over all fractions, that is,

$$D_T(v) = \frac{\sum_{i=1, \dots, K} \varphi_i(E_i)(v)}{M_A(v)} . \quad (3)$$

Equations (1) and (2) are called the MDS and direct dose summation (DDS) methods, respectively. Equation (3) shows that the mass-weighted total dose can be equally defined as the total deposited energy divided by the average mass. The equivalence of the two definitions offers a solution for cross-validation of DDAs.

Figure 1 shows the workflow of the two dose summation methods. Compared to the DDS method illustrated in Figure 1b, the MDS method requires transferring mass to the reference image each time a new dose is added so that the average mass image (M_A) can be updated. Note that in Figure 1, if R is assumed to be one of the source images (X_i), then, the corresponding φ_i will become an identity map.

2.2 | Technical implementation

The MDS method was implemented in an in-house developed dose summation program and demonstrated with CT images acquired from a lung cancer patient for cancer retreatment. The CT scans were acquired in 2017 and 2023 with a Siemens Definition scanner and were used for the development of the initial and retreatment plans, respectively. A CT-to-mass density conversion table was calibrated for this scanner using an advanced electron density phantom (Sun Nuclear Corp, Melbourne, Florida, USA). Based on this table, the CT images were converted to mass images (M_i). The planned doses (D_i) were calculated at each voxel and multiplied by their corresponding mass densities to obtain the amount of the deposited energies (E_i), respectively.

A feature-based, multi-modality DIR algorithm in MIM (MIM Software Inc, Beachwood, Ohio, USA) was employed to register the CT image of 2023 (reference) to that of 2017 (source). The resulting deformation map

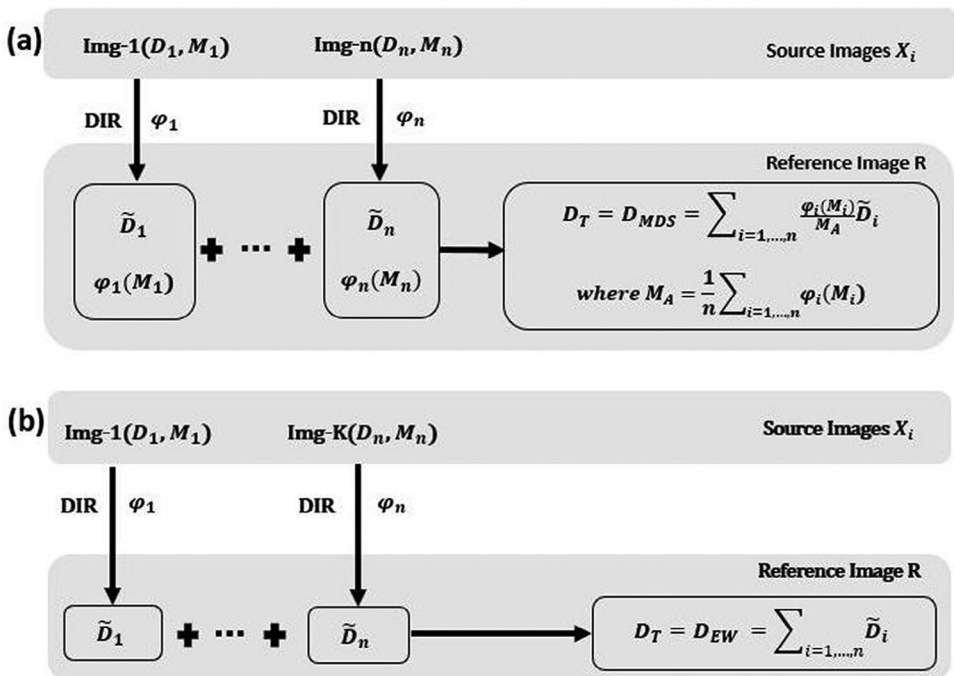


FIGURE 1 The workflow of the deformable dose accumulation methods: (a) mass-weighted dose summation, and (b) direct dose summation.

(φ_i) is defined on the source CT. The images, doses and deformation maps were exported to an in-house program for dose summation. Specifically, energy (E_i) and mass (M_i) were transferred from the source CT to the reference CT using a forward mapping method.¹⁰ With the transferred energy and mass images, the deformed doses (\tilde{D}_i) were reconstructed using the EMC dose reconstruction method and then directly summed using Equation (2) to derive the accumulated dose distribution D_{DDS} . The transferred energy images were summed to generate the accumulated energy image (E_T), and the transferred mass images were averaged to generate the mass average (M_A). Their ratio represents the accumulated dose distribution D_{MDS} , as illustrated in Equation (1).

2.3 | Evaluation

The two dose summation methods were evaluated based on the total treatment energy deposited in individual organs. Since the accumulated doses D_{MDS} and D_{DDS} are defined on the mass of the average and reference images, respectively, their corresponding energies, E_{MDS} and E_{DDS} , can be calculated by multiplying D_{MDS} and D_{DDS} by their respective masses. On the other hand, the accumulated energy E_T is summed directly from the deformed energy images without undergoing any dose summation. D_{MDS} and D_{DDS} can then be evaluated by comparing E_{MDS} and E_{DDS} with E_T for each organ delineated on the reference image.

3 | RESULTS

3.1 | Energy change in MDS and DDS

The lung cancer patient was initially treated with 60 Gy over 30 fractions, followed by a retreatment regimen of 44 Gy delivered in 22 fractions. Mass images were calculated from the two CT scans obtained for the initial and retreatment plans. These mass images were then multiplied by the doses of the two plans to generate their respective energy images. With the replanning CT taken as the reference, an MIM registration was performed between the initial planning CT and the reference CT to generate a deformation map φ_1 . The map φ_1 and an identity map φ_2 were then utilized to transfer energy and mass from the initial and replanning CTs to the reference CT. The transferred mass images $\varphi_1(M_1)$ and $\varphi_2(M_2)$ are shown in Figure 2a and b, respectively. The average of the two mass images is illustrated in Figure 2c. These mass images are represented in the unit of g/cm³ as illustrated by the grey bars in Figure 2a-c. Notably, the densities of lung tissue in the marked tumor region changed after the initial treatment. The transferred energy distributions $\varphi_1(E_1)$ and $\varphi_2(E_2)$ are displayed in Figure 2d and e, respectively, with their combination shown in Figure 2f. The mass difference between the tumor and surrounding lung tissue results in an islanded energy distribution around the tumor for the initial treatment plan, as depicted in Figure 2d.

The EMC method was employed to reconstruct the doses of the initial and retreatment plans on the

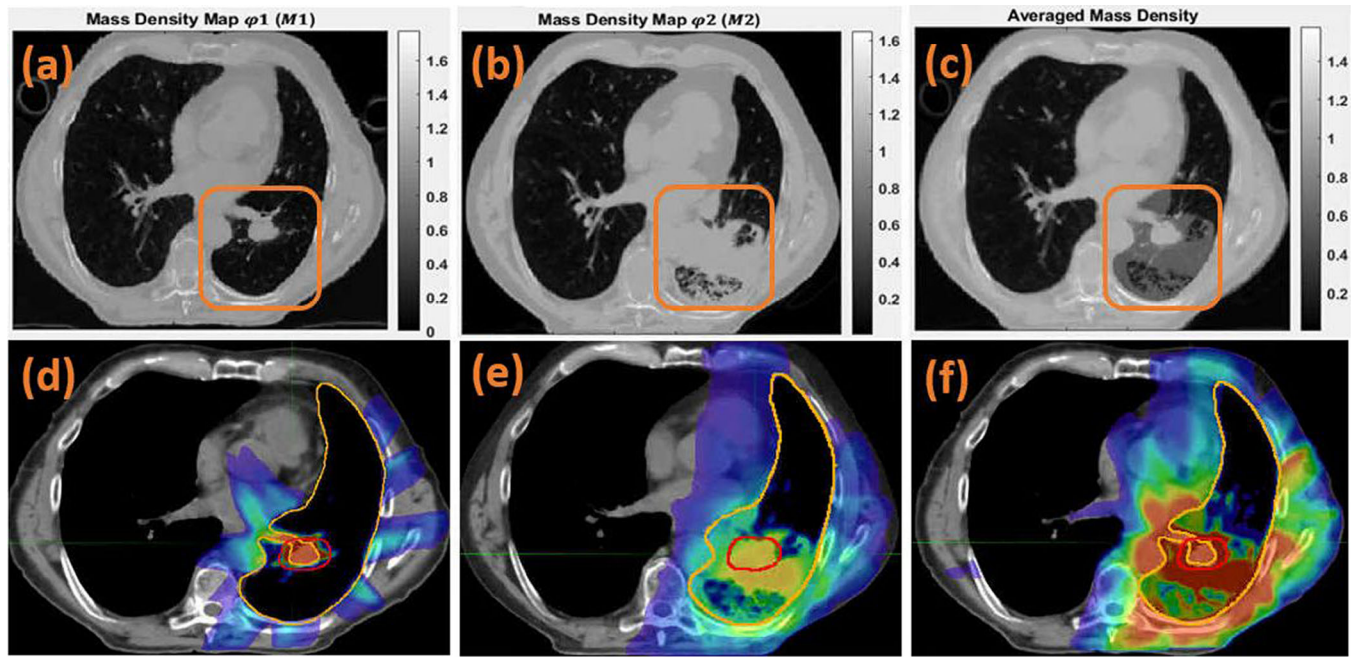


FIGURE 2 Lung cancer patient retreatment: (a) and (b) show the mass images of the initial treatment and retreatment plans, transferred to the reference image; (c) the average of the transferred mass images; (d) and (e) the transferred energy and mass images overlaid for the initial treatment and retreatment plans, respectively; (f) the combination of the transferred energy images shown in (d) and (e). In (d-f), the PTV and left lung contours in the initial treatment plan were mapped to the reference image and illustrated in red and yellow, respectively.

TABLE 1 The energies E_{MDS} and E_{DDS} benchmarked against the directly combined energy E_T .

OAR	Bronchus-L	Esophagus	Heart	Lung-L	V-Pulm	PTV
$(S_{MDS} - S_T)/S_T (\%)$	0.14	0	0.11	0.17	0.02	0.18
$(S_{DDS} - S_T)/S_T (\%)$	2.39	0.13	0.51	11.19	2.50	41.80

reference image. Subsequently, the DDS and MDS methods were used to generate the combined doses, D_{DDS} and D_{MDS} , which were multiplied by the mass of the reference image to derive two energy images, E_{DDS} and E_{MDS} . The E_{DDS} and E_{MDS} were integrated over all voxels in organ j , with the resultant sums denoted by $S_{DDS}(j)$ and $S_{MDS}(j)$, respectively. Meanwhile, the transferred energy images $\varphi_1(E_1)$ and $\varphi_2(E_2)$ were added together to generate the accumulated energy image E_T , which was integrated over all voxels in organ j , with the sum denoted by $S_T(j)$. Finally, $S_{DDS}(j)$ and $S_{MDS}(j)$ were compared to $S_T(j)$, with results listed in Table 1.

The energy image E_{DDS} calculated from D_{DDS} largely differs from the directly combined energy image E_T , exhibiting a mean difference of up to 41.8% in the PTV and 11.2% in the left lung. In contrast, the energy image E_{MDS} calculated from D_{MDS} aligns closely with E_T , with their mean differences within 0.18% for all OARs. The minor difference between E_{MDS} and E_T could be attributed to rounding errors in the computation of mass and energy conversion and summation processes.

3.2 | Dose comparison between MDS and DDS

With the DDS and MDS methods, the doses from the initial and retreatment plans were combined to generate the total dose D_{DDS} on the replanning CT (Figure 3a) and the total dose D_{MDS} on the average CT (Figure 3b), respectively. The 24, 60, and 90 Gy isodose lines of D_{DDS} and D_{MDS} are displayed in purple, green, and yellow. These isodose lines are nearly identical in regions such as the chest wall and heart, but noticeable dose differences can be observed in the lung and tumor regions, where mass changes are significant after the initial treatment.

The means of D_{DDS} and D_{MDS} were calculated for the relevant organs listed in Table 2. The two summed doses differ by 10.2% in the PTV, 14.55% in the left lung, and 1.78% in the esophagus. The dose difference in the esophagus could be attributed to changes in air content. Without mass changes, the two dose summation methods show high consistencies, as demonstrated in other OARs.

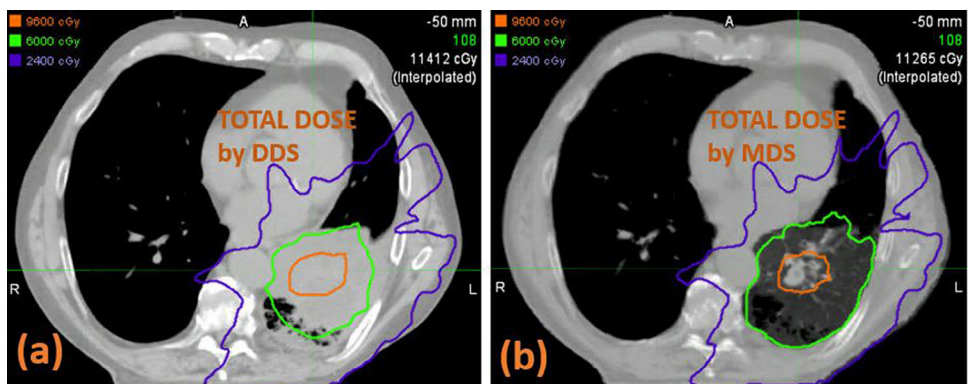


FIGURE 3 Dose comparison between MDS and DDS: (a) isodose lines of D_{DDS} overlaid on the reference image; (b) isodose lines of D_{MDS} overlaid on the average image.

TABLE 2 The means of D_{DDS} and D_{MDS} compared in different organs.

OARs	Bronchus-L	Esophagus	Heart	Lung-L	V-Pulg	PTV
$D_{\text{DDS}}(\text{cGy})$	1476	799	1675	2590	4034	8071
$D_{\text{MDS}}(\text{cGy})$	1486	785	1685	3031	4013	8990
Difference (%)	0.67	1.78	0.59	14.55	0.52	10.22

4 | DISCUSSION

Adaptive radiotherapy requires calculating the total dose for plan evaluation and treatment outcome assessment.¹⁸ Since the effectiveness of adaptive radiotherapy ultimately depends on the total amount of radiation energy deposited in tumor targets and surrounding organs, the calculated total dose should correspond to the total deposited energy in each organ.¹⁵ Unlike non-adaptive radiotherapy, which is planned on a static mass image where calculated dose and energy are mutually convertible, adaptive radiotherapy involves treatment plans developed on different images. Unfortunately, the conventional DDS method cannot account for the mass differences among these images. For instance, if a voxel's mass density is reduced to zero, adding another fractional dose with DDS will increase the total dose while the total energy deposited in that voxel remains unchanged. Thus, the DDS-derived total dose does not correspond to the total deposited energy in organs experiencing mass changes.

Mass changes can occur in various clinical scenarios, such as lung tissue fibrosis, tumor and parotid gland shrinkage, stomach and bladder content variation, or organ growth in pediatric patients. Since treatment outcome depends on the total energy deposited in each organ, the lack of correspondence between the DDS-derived total dose and the total deposited energy compromises the reliability of using the DDS-derived total dose for treatment outcome assessment. In contrast, as shown in Equation (3), the MDS-calculated total dose is defined in terms of the total deposited energy,

accurately reflecting the physics quantity relevant to treatment.

Given that the goal of dose accumulation is to determine the total dose that corresponds to the total deposited energy—not just its portion in the remaining mass—both dose mapping and dose summation should preserve energy so that the final total dose accurately represents the total energy originally deposited in each organ, a fixed quantity independent of subsequent mass changes. Based on its definition in Equation (3), the MDS-derived total dose represents the total deposited energy, even if mass changes occur after energy deposition. The clinical implementation results in Table 1 show that the MDS-induced energy changes are less than 0.18% for all OARs.

The DDS- and MDS-cumulated doses differ primarily in regions experiencing mass changes. As demonstrated in Figure 3a and b, their isodose lines are nearly identical in solid tissues but exhibit significant differences in the left lung, where mass densities changed notably after the initial treatment. Unlike the DDS-derived total dose, which lacks a direct connection to the reference image's mass (Figure 3a), the MDS-derived total dose represents the total energy deposited on the average image's mass, as illustrated in Figure 3b.

Due to concerns about DIR and dose mapping uncertainties, as well as the lack of reliable metrics to detect these uncertainties, DDA is not yet routinely used in clinical practice.¹⁹ However, the deposited energies can be integrated within each organ and summed over all fractions. Based on the equivalent definition of the total dose shown in Equation (3), the summed energy can

serve as a gold standard to verify the accumulated dose in each organ. This method directly verifies the energy of the accumulated dose, fundamentally differing from empirical error metrics such as inverse consistency²⁰ or the Jacobian determinant.²¹ It should be mentioned that since clinical dose limits on OARs are derived according to DDS-cumulated doses,²² these limits may need to be reevaluated if MDS is implemented in clinical practice for dose summation.

5 | CONCLUSION

The total dose generated by the MDS method accurately reflects the total deposited energy, directly correlating with treatment outcomes. This consistency may provide a robust foundation for verifying dose accumulation in adaptive radiotherapy.

ACKNOWLEDGMENTS

This study was funded in part by the grant R01-EB032680 from National Institute of Biomedical Imaging and Bioengineering, NIH.

CONFLICT OF INTEREST STATEMENT

The author declare no conflicts of interest.

DATA AVAILABILITY STATEMENT

The dataset generated and analyzed during the current study are available from the corresponding author on reasonable request.

REFERENCES

- McDonald BA, Zachiu C, Christodouleas J, et al. Dose accumulation for MR-guided adaptive radiotherapy: from practical considerations to state-of-the-art clinical implementation. *Front Oncol.* 2023;12. doi:[10.3389/fonc.2022.1086258](https://doi.org/10.3389/fonc.2022.1086258)
- Thirion JP. Image matching as a diffusion process: an analogy with Maxwell's demons. *Med Image Anal.* 1998;2(3):243-260. doi:[10.1016/S1361-8415\(98\)80022-4](https://doi.org/10.1016/S1361-8415(98)80022-4)
- Rueckert D, Aljabar P, Heckemann RA, Hajnal JV, Hammers A. Diffeomorphic registration using B-splines. *Med Image Comput Comput Assist Interv.* 2006;9(Pt 2):702-709. doi:[10.1007/11866763_86](https://doi.org/10.1007/11866763_86)
- Al-Mayah A, Moseley J, Brock KK. Contact surface and material nonlinearity modeling of human lungs. *Phys Med Biol.* 2008;53(1):305-317. doi:[10.1088/0031-9155/53/1/022](https://doi.org/10.1088/0031-9155/53/1/022)
- Zhong H, Wen N, Gordon JJ, Elshaikh MA, Movsas B, Chetty IJ. An adaptive MR-CT registration method for MRI-guided prostate cancer radiotherapy. *Phys Med Biol.* 2015;60(7):2837-2851. doi:[10.1088/0031-9155/60/7/2837](https://doi.org/10.1088/0031-9155/60/7/2837)
- Shi L, Chen Q, Barley S, et al. Benchmarking of deformable image registration for multiple anatomic sites using digital data sets with ground-truth deformation vector fields. *Pract Radiat Oncol.* 2021;11(5):404-414. doi:[10.1016/j.prro.2021.02.012](https://doi.org/10.1016/j.prro.2021.02.012)
- Rosu M, Chetty IJ, Balter JM, Kessler ML, McShan DL, Ten Haken RK. Dose reconstruction in deforming lung anatomy: dose grid size effects and clinical implications. *Med Phys.* 2005;32(8):2478-2495. doi:[10.1118/1.1949749](https://doi.org/10.1118/1.1949749)
- Heath E, Seuntjens J. A direct voxel tracking method for four-dimensional Monte Carlo dose calculations in deforming anatomy. *Med Phys.* 2006;33(2):434-445. doi:[10.1118/1.2163252](https://doi.org/10.1118/1.2163252)
- Siebers JV, Zhong H. An energy transfer method for 4D Monte Carlo dose calculation. *Med Phys.* 2008;35(9):4096-4105. doi:[10.1118/1.2968215](https://doi.org/10.1118/1.2968215)
- Zhong H, Siebers JV. Monte Carlo dose mapping on deforming anatomy. *Phys Med Biol.* 2009;54(19):5815-5830. doi:[10.1088/0031-9155/54/19/010](https://doi.org/10.1088/0031-9155/54/19/010)
- Li HS, Zhong H, Kim J, et al. Direct dose mapping versus energy/mass transfer mapping for 4D dose accumulation: fundamental differences and dosimetric consequences. *Phys Med Biol.* 2014;59(1):173-188. doi:[10.1088/0031-9155/59/1/173](https://doi.org/10.1088/0031-9155/59/1/173)
- Ziegenhein P, Kamerling CP, Fast MF, Oelfke U. Real-time energy/mass transfer mapping for online 4D dose reconstruction. *Sci Rep.* 2018;8(1):3662. doi:[10.1038/s41598-018-21966-x](https://doi.org/10.1038/s41598-018-21966-x)
- Zhong H, Garcia-Alvarez JA, Kainz K, et al. Development of a multi-layer quality assurance program to evaluate the uncertainty of deformable dose accumulation in adaptive radiotherapy. *Med Phys.* 2023;50(3):1766-1778. doi:[10.1002/mp.16137](https://doi.org/10.1002/mp.16137)
- Bosma LS, Zachiu C, Ries M, Denis De Senneville B, Raaymakers BW. Quantitative investigation of dose accumulation errors from intra-fraction motion in MRgRT for prostate cancer. *Phys Med Biol.* 2021;66(6):065002. doi:[10.1088/1361-6560/abe02a](https://doi.org/10.1088/1361-6560/abe02a)
- Zhong H, Chetty IJ. Adaptive radiotherapy for NSCLC patients: utilizing the principle of energy conservation to evaluate dose mapping operations. *Phys Med Biol.* 2017;62(11):4333-4345. doi:[10.1088/1361-6560/aa54a5](https://doi.org/10.1088/1361-6560/aa54a5)
- Wu X, Amstutz F, Weber DC, Unkelbach J, Lomax AJ, Zhang Y. Patient-specific quality assurance for deformable IMRT/IMPT dose accumulation: proposition and validation of energy conservation based validation criterion. *Med Phys.* 2023;50(11):7130-7138. doi:[10.1002/mp.16564](https://doi.org/10.1002/mp.16564)
- Käsmann L, Niyazi M, Blanck O, et al. Predictive and prognostic value of tumor volume and its changes during radical radiotherapy of stage III non-small cell lung cancer: a systematic review. *Strahlenther Onkol.* 2018;194(2):79-90. doi:[10.1007/s00066-017-1221-y](https://doi.org/10.1007/s00066-017-1221-y)
- Zhong H, Pursley JM, Rong Y. Deformable dose accumulation is required for adaptive radiotherapy practice. *J Appl Clin Med Phys.* 2024;25(8):e14457. doi:[10.1002/acm2.14457](https://doi.org/10.1002/acm2.14457)
- Glide-Hurst CK, Lee P, Yock AD, et al. Adaptive radiation Therapy (ART) strategies and technical considerations: a state of the ART review from NRG oncology. *Int J Radiat Oncol Biol Phys.* 2021;109(4):1054-1075. doi:[10.1016/j.ijrobp.2020.10.021](https://doi.org/10.1016/j.ijrobp.2020.10.021)
- Hardcastle N, Bender ET, Tomé WA. The effect on dose accumulation accuracy of inverse-consistency and transitivity error reduced deformation maps. *Australas Phys Eng Sci Med.* 2014;37(2):321-326. doi:[10.1007/s13246-014-0262-0](https://doi.org/10.1007/s13246-014-0262-0)
- Vickress J, Battista J, Barnett R, Yartsev S. Representing the dosimetric impact of deformable image registration errors. *Phys Med Biol.* 2017;62(17):N391-N403. doi:[10.1088/1361-6560/aa8133](https://doi.org/10.1088/1361-6560/aa8133)
- Embring A, Onjukka E, Mercke C, et al. Re-irradiation for head and neck cancer: cumulative dose to organs at risk and late side effects. *Cancers (Basel).* 2021;13(13):3173. doi:[10.3390/cancers13133173](https://doi.org/10.3390/cancers13133173)

How to cite this article: Zhong H. An energy-conserving dose summation method for dose accumulation in radiotherapy. *Med Phys.* 2025;52:1305-1310.

<https://doi.org/10.1002/mp.17514>